REPORT DOCUMENTATION PAGE

Form Approved
OMB No. 0704-0188

1. AGENCY USE ONLY (Leave Blank)	2. REPORT DATE	3. REPORT TYPE AND DATES COVERED
	22 MAY 1996	PROFESSIONAL PAPER

4. TITLE AND SUBTITLE

SIMULATION VALIDATION THROUGH LINEAR MODEL COMPARISON

5. FUNDING NUMBERS

6. AUTHOR(S)

KEITH BALDERSON, DONALD P. GAUBLOMME, AND JUSTIN W. THOMAS

7. PERFORMING ORGANIZATION NAMES(S) AND ADDRESS(ES)

COMMANDER
NAVAL AIR WARFARE CENTER AIRCRAFT DIVISION
22541 MILLSTONE ROAD
PATUXENT RIVER, MARYLAND 20670-5304

8. PERFORMING ORGANIZATION REPORT NUMBER

9. SPONSORING / MONITORING AGENCY NAME(S) AND ADDRESS(ES)

COMMANDER
NAVAL AIR SYSTEMS COMMAND
1421 JEFFERSON DAVIS HIGHWAY
ARLINGTON, VA 22243

10. SPONSORING / MONITORING AGENCY REPORT NUMBER

11. SUPPLEMENTARY NOTES

12a. DISTRIBUTION / AVAILABILITY STATEMENT

APPROVED FOR PUBLIC RELEASE; DISTRIBUTION UNLIMITED.

12b. DISTRIBUTION CODE

13. ABSTRACT (Maximum 200 words)

The Manned Flight Simulator at the Naval Air Warfare Center in Patuxent River, MD maintains high fidelity fixed and rotary wing simulation models. The aircraft simulations are utilized for a wide range of activities including flight test support, pilot training, and control law analysis and design. Validating aircraft math models against flight test data is an important part of the simulation process. Linear model comparison was used to validate the lateral-directional dynamic modes of the V-22 tilt-rotor aircraft in airplane mode. In this technique, linear model approximations of the simulation and aircraft dynamics are calculated independently and then compared. The simulation linear state-space model was extracted from the nonlinear V-22 simulation using a perturbation method. The aircraft linear state-space model was fit to flight test data from lateral-directional maneuvers using parameter identified tools. Time history comparison were used to verify both linear models. Comparison of the lateral-directional modes and the stability and control derivatives of the two models were made. The differences between the two models were used to locate potential problems with the nonlinear simulation.

14. SUBJECT TERMS
V-22; tilt-rotor; lateral-directional

15. NUMBER OF PAGES
11

16. PRICE CODE

17. SECURITY CLASSIFICATION OF REPORT	18. SECURITY CLASSIFICATION OF THIS PAGE	19. SECURITY CLASSIFICATION OF ABSTRACT	20. LIMITATION OF ABSTRACT
UNCLASSIFIED	UNCLASSIFIED	UNCLASSIFIED	N/A

NSN 7540-01-280-5500

Standard Form 298 (Rev. 2-89)
Prescribed by ANSI Std. Z39-18
298-102

Encl (6)

SIMULATION VALIDATION THROUGH LINEAR MODEL COMPARISON

Keith A. Balderson*

Donald P. Gaublomme†

Naval Air Warfare Center Aircraft Division
Code 432200A, MS-3
48140 Standley Road
Patuxent River, Maryland 20670

Justin W. Thomas‡

Science Applications International Corporation
Systems Technology Group
44417 Pecan Court, Suite B
California, Maryland 20619

Abstract

The Manned Flight Simulator at the Naval Air Warfare Center in Patuxent River, MD maintains high fidelity fixed and rotary wing simulation models. The aircraft simulations are utilized for a wide range of activities including flight test support, pilot training, and control law analysis and design. Validating aircraft math models against flight test data is an important part of the simulation process. Linear model comparison was used to validate the lateral-directional dynamic modes of the V-22 tilt-rotor aircraft in airplane mode. In this technique, linear model approximations of the simulation and aircraft dynamics are calculated independently and then compared. The simulation linear state-space model was extracted from the nonlinear V-22 simulation using a perturbation method. The aircraft linear state-space model was fit to flight test data from lateral-directional maneuvers using parameter identification tools. Time history comparisons were used to verify both linear models. Comparisons of the lateral-directional modes and the stability and control derivatives of the two models were made. The differences between the two models were used to locate potential problems with the nonlinear simulation.

Nomenclature

a_{1L}	Left rotor longitudinal flapping (deg)
a_{1R}	Right rotor longitudinal flapping (deg)
b_{1L}	Left rotor lateral flapping (deg)
b_{1R}	Right rotor lateral flapping (deg)
A	State-space system matrix
B	State-space control matirix
C	State-space output matrix
C_l	Nondimensional roll moment coefficient
C_N	Nondimensional yaw moment coefficient
C_Y	Nondimensional side force coefficient
D	State-space output control matrix
g	Gravity constant (ft/sec^2)
G	Cost function weighting matrix
I_{XX}	Moment of inertia about x body axes (slug-ft^2)
I_{YY}	Moment of inertia about y body axes (slug-ft^2)
I_{ZZ}	Moment of inertia about z body axes (slug-ft^2)
I_{XZ}	Product of inertia about x-z body axes (slug-ft^2)
J	Cost function matrix
L	Roll moment, body axes (ft-lb)
m	Aircraft mass (slug)
N	Yaw moment, body axes (ft-lb)
p	Roll rate perturbation, body axes (rad/sec)
r	Yaw rate perturbation, body axes (rad/sec)
t	Time (sec)
T	Total number of time steps
T_R	Roll mode time constant (sec)
T_S	Spiral mode time constant (sec)
u	State-space input vector
U	x velocity, body axes (ft/sec)
U_{Theil}	Theil coefficient
v	y velocity perturbation, body axes (ft/sec)
W	z velocity, body axes (ft/sec)
x	State-space state vector
y	State-space output vector
Y	Side force, body axes (lb)

* Aerospace Engineer
† Aerospace Engineer
‡ Aerospace Engineer

Greek

β	Angle of sideslip (deg)
δ_a	Aileron position (deg)
δ_r	Rudder position (deg)
Δ	Denotes perturbed value
ζ	Damping ratio
ϕ	Roll attitude perturbation (rad)
Θ	Pitch attitude (rad)
ρ	Air density (slug/ft^3)
ω_n	Undamped natural frequency (rad/sec)

Subscripts

0	At reference flight condition

Superscripts

$\dot{}$	Time rate of change
$\hat{}$	Estimated

Introduction

The V-22 tilt-rotor simulation at the Manned Flight Simulator (MFS) is a high fidelity nonlinear simulation utilized for flight test support, pilot training, and control law analysis. The airframe model is based on the Bell Helicopter Generic Tilt-Rotor simulation. The rotor model is a disk model with dynamic longitudinal and lateral flapping states. The rotor model structure is based on helicopter aerodynamic theory, flight test data, rotor test stand data, blade element model data, and airplane mode propeller efficiency data. The aerodynamic model is a component buildup of the aerodynamic subsystems including the fuselage, wing-pylon, horizontal tail, vertical tail, and landing gear. The aerodynamic model structure and data tables are based on wind tunnel data, theoretical equations, and flight test data.

The V-22 simulation is implemented in the MFS Controls Analysis and Simulation Test Loop Environment (CASTLE). CASTLE is a modular shell structure designed for simulation development, execution, and analysis. The modular design allows CASTLE to support a wide range of rotary and fixed wing aircraft. CASTLE provides a standard looping structure, equations of motion, and atmospheric models, as well as engineering analysis facilities for simulation validation.[1]

The data presented in this paper is part of an ongoing full envelope validation of the V-22 math model against flight test data. Initially, time history comparisons were used to validate the dynamic response of the V-22 simulation in airplane mode. For time history comparison, the simulation inputs are overdriven with flight test data, and the simulation outputs are plotted with measured flight test outputs. If the simulation outputs follow the flight test data within a desired tolerance then the simulation is validated. Overall the nonlinear simulation matched the airplane mode flight test data very well with one exception.

The simulation did not match the flight test data for lateral-directional maneuvers with the flaps set at twenty degrees. For this case, the time history plots alone did not provide enough information to understand the shortcomings of the simulation. The differences between the simulation model and flight test data for these lateral-directional maneuvers were investigated using linear model comparison.

Linear model comparison is a validation technique that provides dynamic mode and stability derivative information which can be used to update the full nonlinear simulation.[2] In this technique, linear model approximations of the simulation and aircraft dynamics are calculated independently and then compared. If the simulation model matches the flight test model within a desired tolerance then the simulation is validated.

A number of techniques are available to extract a linear model from a nonlinear simulation.[3] For this analysis, the simulation linear model was extracted using a perturbation technique. A second linear model representing the aircraft dynamics was fit to flight test data using time domain parameter identification (PID) tools.

Overview of the V-22 Osprey

The V-22 Osprey is a tilt-rotor aircraft capable of flight from hover to high speed airplane mode. Control of the V-22 is accomplished through both conventional airplane and helicopter controls, as illustrated by Figure 1. The airplane controls include an elevator, four flaperons, and two rudders. The helicopter controls include collective pitch, longitudinal cyclic, and lateral cyclic for each rotor.

The V-22 has a digital fly-by-wire control system consisting of a primary flight control system (PFCS) and an automatic flight control system (AFCS). The PFCS provides pilot control input shaping and essential feedback loops. The AFCS is designed to provide Level 1 handling qualities and auto-pilot functions.

In airplane mode, the aircraft is primarily controlled with the aerodynamic control surfaces; however, the

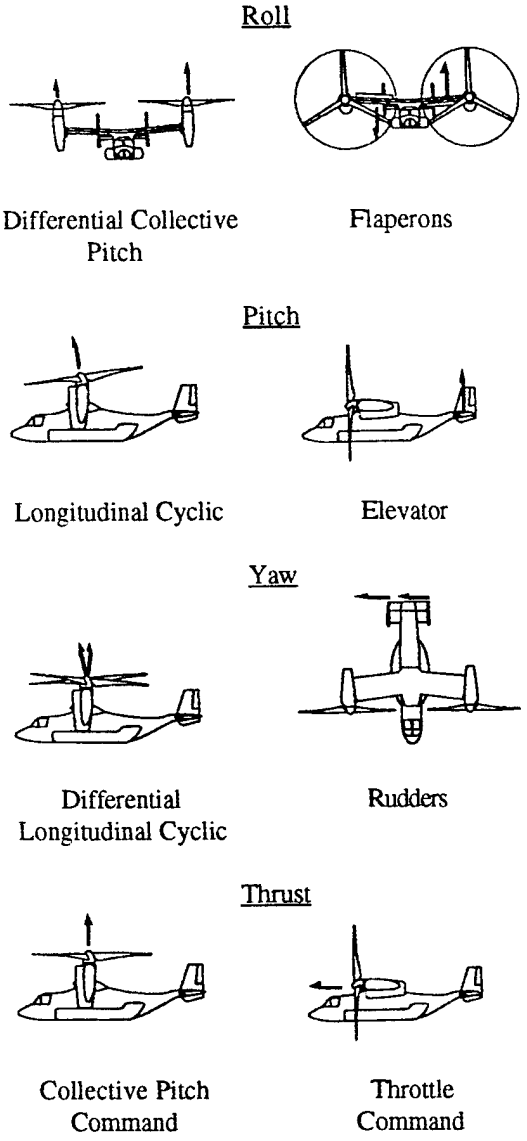

Figure 1. V-22 Controls: Helicopter (Left) and Airplane (Right).

rotor controls are still significant. The PFCS uses the rotor cyclic inputs to minimize the flapping angles of each rotor and the collective inputs to maintain a constant rotor speed and enhance thrust control.

State-Space Model Definition

The models developed in this study utilize a standard continuous time, state-space model.

$$\dot{\mathbf{x}} = A\mathbf{x} + B\mathbf{u} \quad (1)$$
$$\mathbf{y} = C\mathbf{x} + D\mathbf{u} \quad (2)$$
$$\mathbf{x}(t_0) = \mathbf{x}_0 \quad (3)$$

It is common practice to model the lateral-directional dynamics of an aircraft with a fourth order system.[4, 5] Typically in this type of model, the four states are the sideward velocity, roll rate, yaw rate, and roll angle. The inputs to the system are the rudder and aileron deflections.

To develop a linear model based on these states and inputs, the equations of motion for a rigid body are significantly simplified. The small perturbation approach is used to linearize the equations, and the higher order terms are neglected. It is assumed that the lateral-directional and longitudinal equations of motion may be separated.[4] Gyroscopic contributions from the rotors are neglected because the left and right rotors rotate in opposite directions. The lateral-directional dynamic equations are shown below.

$$Y_0 + \Delta Y + mg\phi\cos\Theta_0 = m(\dot{v} - W_0 p + U_0 r) \quad (4)$$
$$L_0 + \Delta L = I_{XX}\dot{p} - I_{XZ}\dot{r} \quad (5)$$
$$N_0 + \Delta N = -I_{XZ}\dot{p} + I_{ZZ}\dot{r} \quad (6)$$
$$\dot{\phi} = p + r\tan\Theta_0 \quad (7)$$

For unaccelerated initial conditions, the initial forces and moments (Y_0, L_0, and N_0) are zero. The perturbation force and moments can each be approximated with a first order Taylor expansion. The partial derivatives, $Y_\bullet$, $L_\bullet$, and $N_\bullet$, are known as the dimensional stability and control derivatives.

$$\Delta Y = Y_v v + Y_p p + Y_r r + Y_{\delta r}\delta_r + Y_{\delta a}\delta_a \quad (8)$$
$$\Delta L = L_v v + L_p p + L_r r + L_{\delta r}\delta_r + L_{\delta a}\delta_a \quad (9)$$
$$\Delta N = N_v v + N_p p + N_r r + N_{\delta r}\delta_r + N_{\delta a}\delta_a \quad (10)$$

The cross-product of inertia, I_{XZ}, for the V-22 is generally less than 1% of the moments of inertia, I_{XX} and I_{ZZ}, so the roll-yaw coupling terms in equations 5 and 6 can be ignored without significantly affecting the model dynamics. This yields the final state equations for the rigid body dynamics.

$$\dot{v} = \frac{Y_v}{m}v + \left(\frac{Y_p}{m} - W_0\right)p + \left(\frac{Y_r}{m} + U_0\right)r + g\cos\Theta_0\phi + \frac{Y_{\delta r}}{m}\delta_r + \frac{Y_{\delta a}}{m}\delta_a \quad (11)$$

$$\dot{p} = \frac{1}{I_{XX}}\left(L_v v + L_p p + L_r r + L_{\delta r}\delta_r + L_{\delta a}\delta_a\right) \quad (12)$$

$$\dot{r} = \frac{1}{I_{ZZ}}\left(N_v v + N_p p + N_r r + N_{\delta_r}\delta_r + N_{\delta_a}\delta_a\right) \quad (13)$$

$$\dot{\phi} = p + r\tan\Theta_0 \quad (14)$$

For the V-22, additional states and inputs are required to model the dynamics of the rotor system. The states are the longitudinal and lateral flapping angles, and the inputs are the longitudinal and lateral cyclic pitch angles and the collective pitch angles.

Combining the rotor and rigid body dynamic models generates an 8th order state-space system. The A matrix can be divided into four quadrants as shown below, where the diagonal quadrants contain the pure rigid body and rotor dynamics, and the off diagonal quadrants represent the cross-coupling of the two systems.

$$A_{total} = \left[\begin{array}{c|c} A_{rigid\ body} & A_{rotor\ on\ rigid\ body} \\ \hline A_{rigid\ body\ on\ rotor} & A_{rotor} \end{array}\right] \quad (15)$$

The $A_{rigid\ body}$ quadrant is defined by equations 11-14.

Similarly, the control matrix, B, can be separated into quadrants for the control surface and rotor input effects on the rigid body and rotor states.

$$B_{total} = \left[\begin{array}{c|c} B_{surfaces\ on\ rigid\ body} & B_{rotor\ inputs\ on\ rigid\ body} \\ \hline B_{surfaces\ on\ rotor} & B_{rotor\ inputs\ on\ rotor} \end{array}\right] \quad (16)$$

The upper left quadrant is defined by equations 11-14. Since the rigid body control surfaces have no effect on the rotor flapping, the elements of the lower left quadrant are zeros. The cyclic inputs have very little effect on the rigid body motion, but the collective inputs for each rotor have a significant effect on the yaw rate.

The C matrix is nearly identity since the output vector is approximately equivalent to the state vector. The matrix does contain terms to transform the flapping angles to the axes used in flight test measurements. The D matrix is identically zero since the inputs do not directly affect the outputs.

Linear Model Extraction from the Nonlinear Simulation

The V-22 simulation in the CASTLE architecture was initialized at the flight test initial conditions. The initial conditions were level steady-state flight, nacelles fixed in airplane mode, true velocity of 183 knots, and flaps set at twenty degrees. A linear model was obtained from the full nonlinear simulation using the Linear Model Extraction (LME) facility.[3]

LME uses the offset derivative method to extract a linear model. In this method, perturbations are added to each input and state, and the resulting changes in outputs and state derivatives are recorded. Integration is frozen within the simulation so that the state derivatives are not allowed to propagate. The state-space matrices are then computed.

$$A_{ij} = \frac{\Delta\dot{x}_i}{\Delta x_j} \qquad B_{ik} = \frac{\Delta\dot{x}_i}{\Delta u_k}$$

$$C_{nj} = \frac{\Delta y_n}{\Delta x_j} \qquad D_{nk} = \frac{\Delta y_n}{\Delta u_k} \quad (17)$$

In the above equation, i is the state derivative index, j the state index, k the control input index, and n the output index.

Since the simulation in general is nonlinear, the change in outputs and state derivatives for different size perturbations may not be perfectly linear. The user specifies four perturbation sizes for each input and state. LME perturbs the simulation positively and negatively for each of the perturbation sizes and picks the perturbation size that results in the best linearity. A typical example of an LME result for a linear relationship is shown in Figure 2.

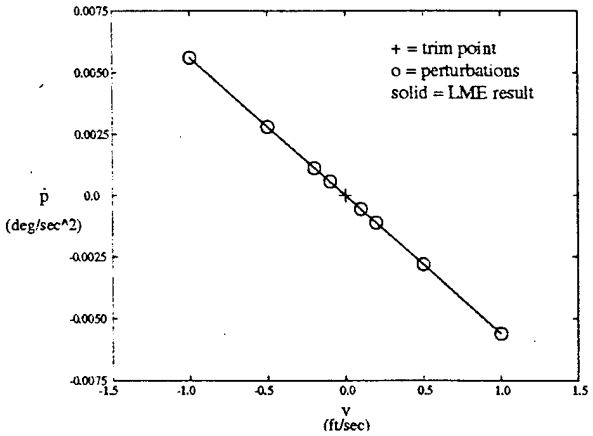

Figure 2. LME result for a linear relationship between the state derivative and perturbation parameter.

In some cases the LME result shows that a linear relationship between an output and a perturbation does not exist. An example of a nonlinear relationship is shown in Figure 3. This figure shows that the linear approximation of the nonlinear data is adequate near the reference condition. The linearity information is useful in determining the quality of the linear model with respect to each coefficient. The output of LME is the state-space model and the linearity information for each coefficient.

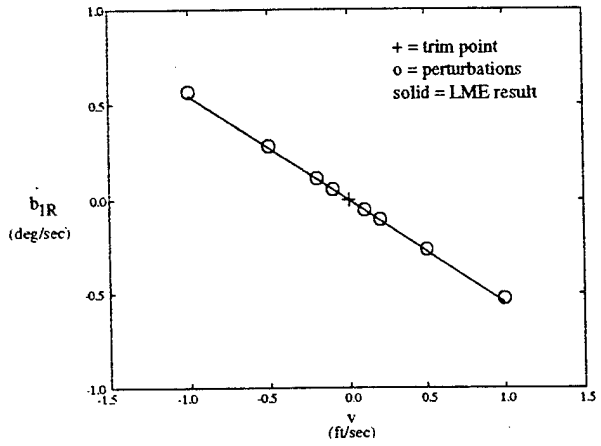

Figure 3. LME result for a nonlinear relationship between the state derivative and perturbation parameter.

Verification of the LME Model

The state-space LME model was compared to the full nonlinear simulation to examine the quality of the extracted linear model. Two input maneuvers, a lateral stick ramp and a rudder doublet, were used to verify the linear model. Each model was driven with the same inputs, and the model outputs were compared. The control inputs and the model outputs are shown in Figure 4 as a concatenated data set. The figure shows that the linear model accurately represents the lateral-directional dynamics of the full nonlinear simulation about the reference flight condition for the two maneuvers.

Linear Model Identification to Flight Test Data

Three lateral-directional flight test maneuvers, a roll reversal, a yaw reversal, and a yaw doublet, were used for the parameter identification. Visual inspection of the 30 degree roll reversal showed good excitation of the roll mode and yaw due to roll characteristics. The yaw reversal and yaw doublet showed good excitation of the dutch roll mode on the sideward velocity and yaw rate time histories. The flight test data was preprocessed and analyzed for kinematic consistency. The final data set showed good consistency with the rigid body kinematic equations. The three maneuvers were concatenated for parameter identification.

Parameter identification was limited to stability and control derivatives from the rigid body lateral-directional equations contained in the upper left hand quadrants of the A and B matrices. No parameters in the rotor dynamic equations or the cross-coupling matrices were included in the identification. Identification of rotor dynamic parameters from maneuvers with mainly conventional airplane control inputs was not attempted. The LME state-space matrices were used as the initial parameter values in the identification.

The parameters available for identification formed a set of nine stability derivatives and six control derivatives. Cramer-Rao bounds, which are estimates of the standard deviation of the identified parameters, were used to assess the identifiability of each parameter.[6] Three stability derivatives and one control derivative had relatively high Cramer-Rao bounds and were not identified. These parameters were held constant at the LME model value.

The cost function was defined as a weighted sum of squared errors between the measured outputs, $\mathbf{y}$, and the estimated outputs, $\hat{\mathbf{y}}$. The weighting matrix, G, is a diagonal matrix that contains the relative weighting for each output.

$$J = \sum_{i=1}^{T} \left[G(\mathbf{y}_i - \hat{\mathbf{y}}_i)^2 \right] \tag{18}$$

The rigid body states were weighted ten times greater than the rotor flapping states for the identification. The rotor flapping outputs were included in the cost function because the rigid body equations and rotor dynamic equations are coupled.

The cost function was minimized through parameter identification using the MATLAB® computing environment. The state-space model was overdriven with flight test inputs to produce the estimated outputs. A Levenburg-Marquardt routine, which is a combination of the Gauss-Newton and steepest descent methods, was used to minimize the cost function.[7]

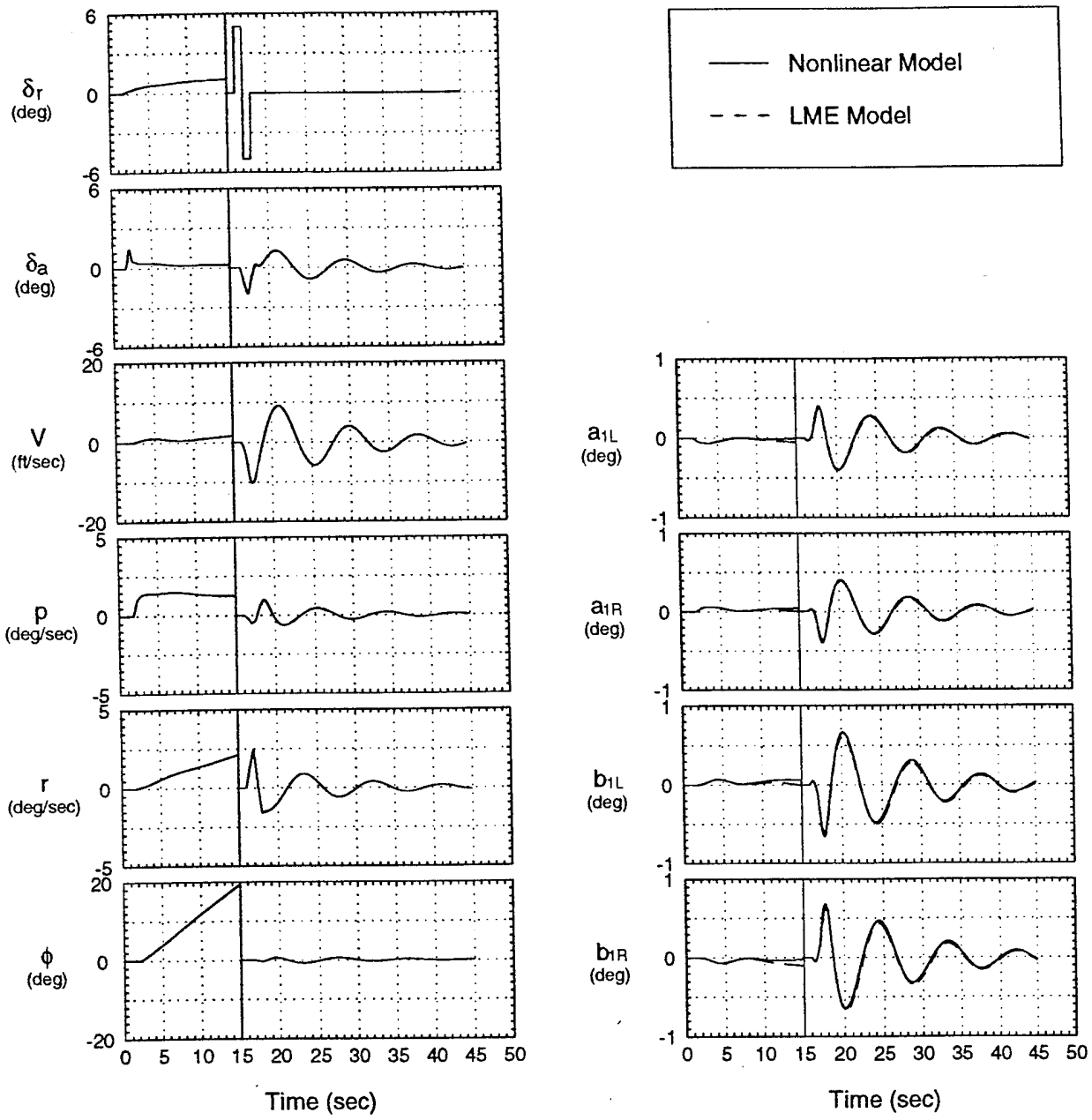

Figure 4. Verification of the LME model to the full nonlinear simulation.

The measured inputs and outputs from flight test, the LME model outputs, and the PID model outputs are shown in Figure 5. A marked improvement in the identified model is evident from the plots of the outputs.

The improvement of the identification was quantitatively assessed using goodness of fit statistics applied to the measured and modeled outputs. Theil's inequality coefficient is a statistic that scales the root mean square error between zero and one. An inequality coefficient value of zero indicates a perfect fit, and a value of one indicates the fit is as bad as possible.[8]

$$U_{Theil} = \frac{\sqrt{\frac{1}{T}\sum_{i=1}^{T}(\mathbf{y}_i - \hat{\mathbf{y}}_i)^2}}{\sqrt{\frac{1}{T}\sum_{i=1}^{T}(\mathbf{y}_i)^2} + \sqrt{\frac{1}{T}\sum_{i=1}^{T}(\hat{\mathbf{y}}_i)^2}} \tag{19}$$

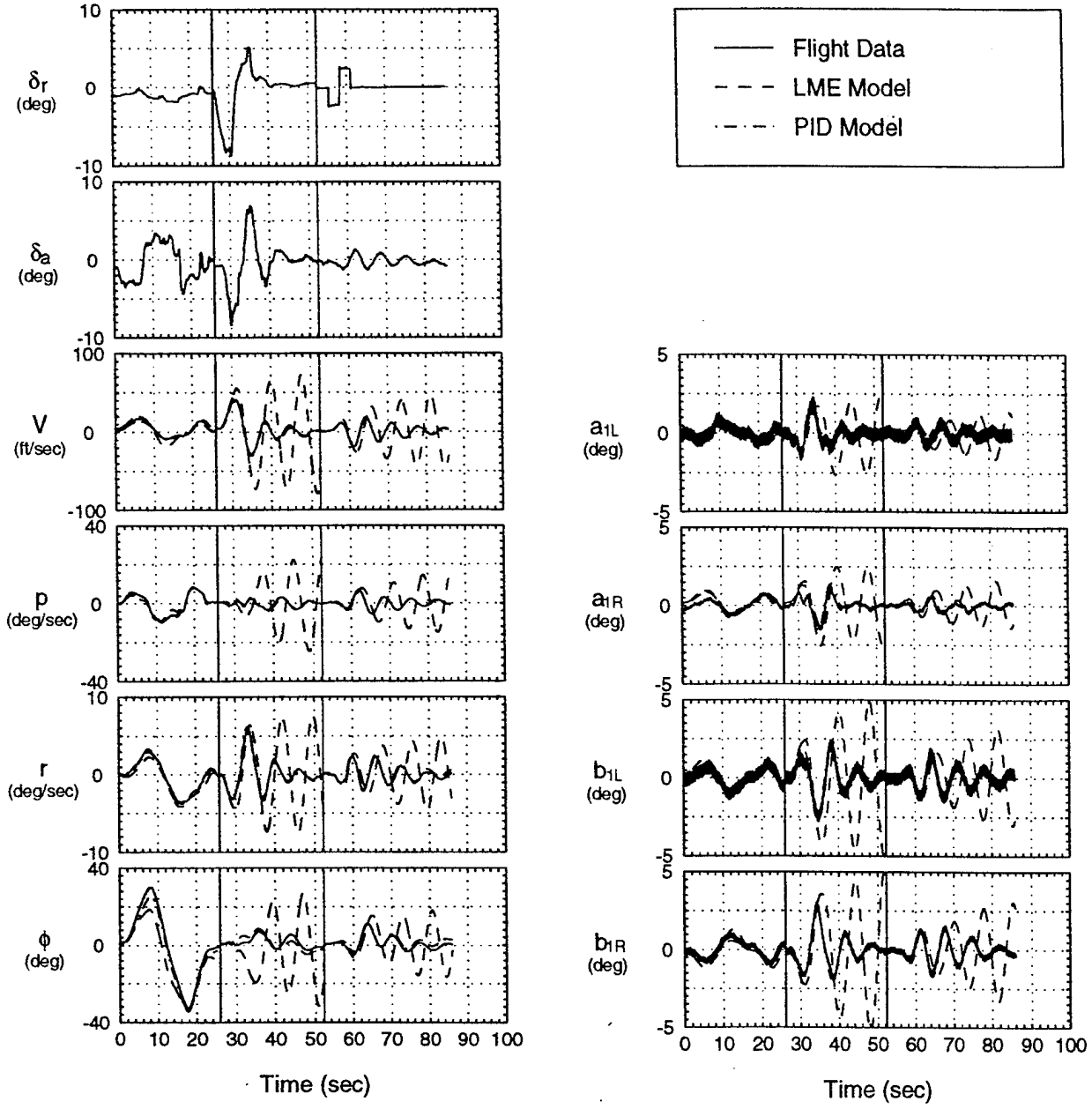

Figure 5. Flight test data and LME and PID model outputs for the parameter identification maneuvers.

Goodness of fit statistics showing the improvement from the initial model to the identified model are presented in the first part of Table 1.

Verification of the PID Model

The PID state-space model was verified against independent flight test data to assess the quality of the model. Often a model will match the data used in the identification but will not accurately predict independent data. Good prediction capability provides confidence that the identified model represents the actual aircraft dynamics.

A yaw doublet not included in the identification was used to verify the identified model. The identified model was overdriven with the inputs from the yaw doublet and the outputs were compared to the flight test data. Figure 6 shows the flight test and model outputs.

Table 1. Goodness of fit statistics comparing the LME outputs and the PID model outputs to flight test data used in the identification and independent verification data.

State Space Model Outputs	U_{Theil} LME Model Identification Data Set	U_{Theil} PID Model Identification Data Set	U_{Theil} PID Model Verification Data Set
v	0.679	0.079	0.210
p	0.742	0.072	0.256
r	0.586	0.079	0.227
ϕ	0.491	0.094	0.293
a_{1R}	0.674	0.388	0.411
a_{1L}	0.685	0.310	0.345
b_{1L}	0.728	0.223	0.217
b_{1R}	0.723	0.145	0.255

The PID model adequately represents the verification data at the beginning of the maneuver while the rudder doublet is active. The model is somewhat overdamped during the remainder of the maneuver. Goodness of fit statistics for the verification yaw doublet are presented in the last column of Table 1. As expected, the Theil coefficients for the verification data set are higher than those for the identification data set, but they still show an improvement over the initial LME model.

The identification process produced a state-space model with adequate dutch roll prediction capability. Less confidence was placed in the roll mode predictability for two reasons. The thirty degree roll reversal used in the identification stretches the linearity assumption, and independent flight test data was not available to verify the roll response.

Comparison of Linear Models

An obvious conclusion that could be drawn from Figure 5 is that the LME state-space model does not accurately represent the dutch roll mode of the aircraft. The time history plots for the yaw reversal from the LME model suggest a slightly unstable dutch roll mode. Quantifying this problem using only a time history comparison would be very difficult.

An inherent strength of the linear model comparison method is the ability to compare the dynamic modes

Table 2. Lateral-directional dynamic stability characteristics for the LME and PID models.

	Dutch Roll Mode		Spiral Mode	Roll Mode
	ζ	ω_N	T_S	T_R
LME Model	-0.004	0.820	7.94	1.26
PID Model	0.041	1.005	8.87	1.37

Table 3. Nondimensional stability derivative values from the LME and PID models.

Stability Derivative	LME Model	PID Model	Difference
$C_{Y\beta}$	-2.41	-2.42	-0.01
C_{Yp}	-0.464	-0.464	No ID
C_{Yr}	0.506	0.506	No ID
$C_{Y\delta r}$	-0.236	-0.240	-0.004
$C_{Y\delta a}$	-0.226	-0.226	No ID
$C_{l\beta}$	-0.342	-0.406	-0.064
C_{lp}	-1.20	-1.18	0.02
C_{lr}	-0.169	-0.169	No ID
$C_{l\delta r}$	-0.017	-0.072	-0.055
$C_{l\delta a}$	-0.350	-0.320	0.030
$C_{N\beta}$	0.042	0.138	0.096
C_{Np}	-0.640	-0.683	-0.043
C_{Nr}	-1.77	-1.85	-0.08
$C_{N\delta r}$	0.173	0.159	-0.014
$C_{N\delta a}$	-0.0217	-0.0400	-0.0183

contained in the state-space models. The eigenvalues of the A matrix which describe the modes of the aircraft are easily calculated in MATLAB®. The eigenvalues of the lateral-directional rigid body equations are shown on a complex plane plot in Figure 7. The damping ratio and undamped natural frequency of the dutch roll mode, along with the time constants of the spiral and roll modes, are shown in Table 2. The acceptable tolerance

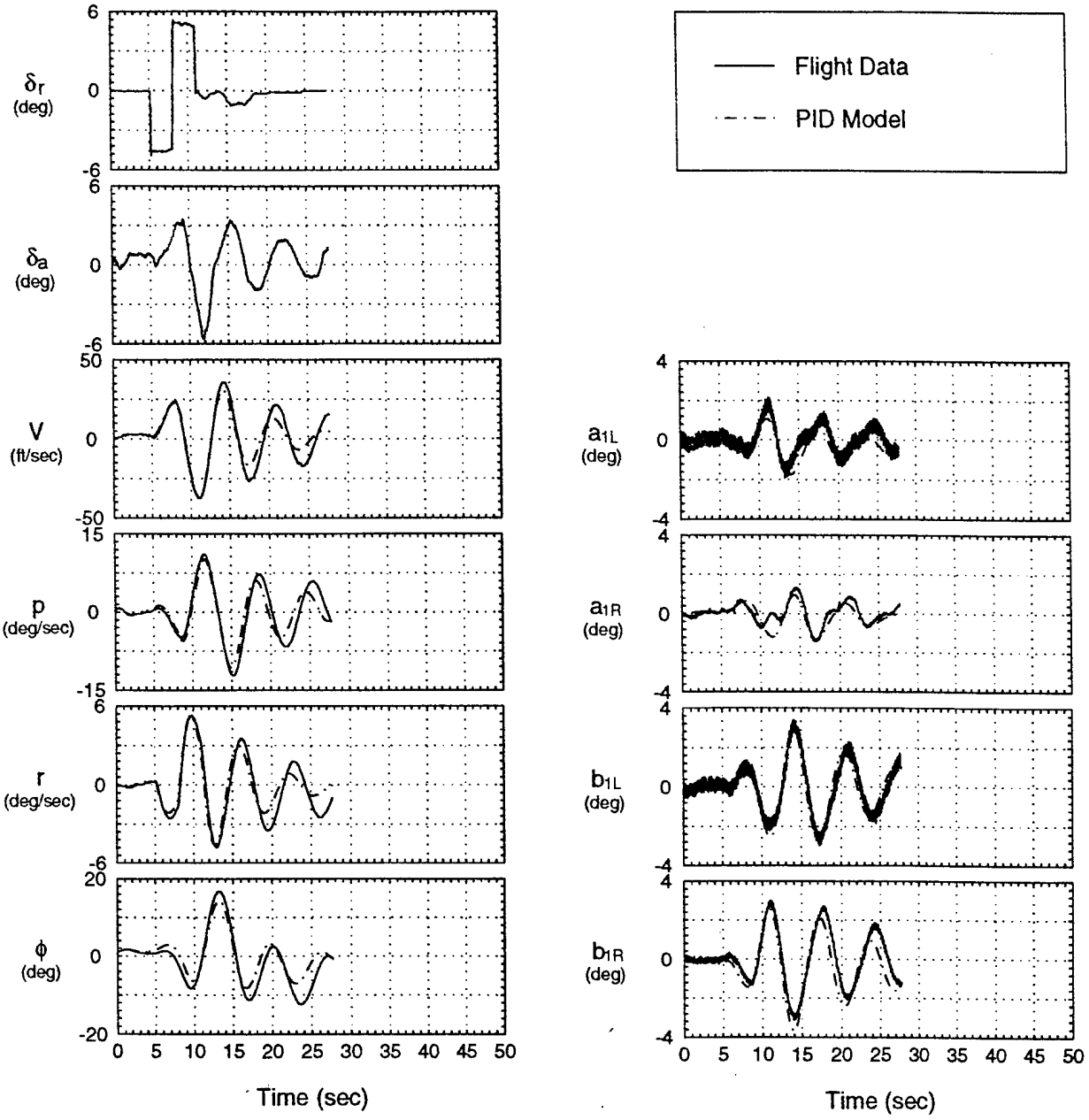

Figure 6. Flight test data and PID model outputs for an independent verification yaw doublet.

for error in the mode comparison depends on the specific aircraft and simulation application. A general tolerance of 5% has been proposed for this type of analysis.[2]

Both the LME and PID models contain classic second order dutch roll modes. The dutch roll mode of the LME model is slightly unstable as evident from the negative damping ratio. The dutch roll damping ratio of the identified model is larger in magnitude and positive. The LME dutch roll natural frequency is 18% less than the dutch roll natural frequency of the PID model. Based on the proposed tolerance, the LME model is not a valid representation of the dutch roll mode exhibited in flight test.

The LME and PID models both contain first order spiral and roll modes. The spiral mode time constant of the LME model is 10% less than that of the PID model. The roll mode time constant of the LME model is 8% less than the PID model value.

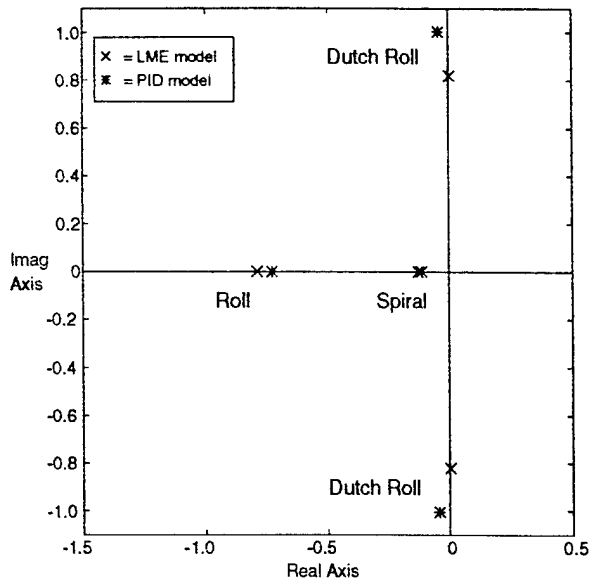

Figure 7. Complex plane plot of the lateral-directional dynamic modes from the LME and the PID models.

In addition to the dynamic mode information, the aircraft stability and control derivatives can be calculated from the state-space models. The dimensional stability derivatives are imbedded in the elements of the state-space model as shown in equations 11-13. The rigid body stability and control derivatives were extracted from the A and B matrices and nondimensionalized. Table 3 contains the nondimensional stability and control derivatives calculated from the LME and identified models.

Simulation Stability Derivative Investigation

Two approaches can be taken to incorporate the increments in stability and control derivatives into the nonlinear simulation. The most straightforward approach is to directly add the increments into the aerodynamic force and moment equations. This approach is only appropriate for simple simulation models. The nonlinear nature of the V-22 simulation does not lend itself to this direct method. For complex models such as the V-22, the stability and control derivative information can be used to locate weaknesses in the physically based equations of the simulation model.

The shaded stability derivative in Table 3, $C_{N\beta}$, showed the greatest difference between the LME and PID models. $C_{N\beta}$ is the nondimensional yawing moment coefficient due to sideslip. $C_{N\beta}$ must be positive for the aircraft to exhibit directional stability. In the nonlinear simulation, this coefficient contains contributions from the aerodynamic and rotor models. The signs and magnitudes of these contributions can be examined in the LME environment.

Examination of the $C_{N\beta}$ components showed that the rotor model contribution is destabilizing (negative) and the aerodynamic model contribution is stabilizing (positive). The rotor model contribution is only slightly smaller in magnitude than the aerodynamic model contribution. The rotor and aerodynamic models combined to produce a total simulation $C_{N\beta}$ that provides weak directional stability.

Investigation into the rotor model equations showed that the magnitude of the rotor model $C_{N\beta}$ contribution is dependent on a sideward velocity effect model. This sideward velocity effect is intended to model the interference effect that one rotor would have on the other. For high speed airplane mode flight, physical intuition suggests that the interference effect between the rotors should be negligible. Elimination of the sideward velocity effect in the nonlinear simulation decreased the rotor destabilizing effect on the directional stability, and the total $C_{N\beta}$ moved closer to the PID predicted value.

Further investigation is required to determine the history of the sideward velocity effect and assess the validity of the effect for airplane mode flight. In this investigation the linear model comparison technique has provided valuable insight into the validation process and may have located a weakness in the rotor model physical equations.

Conclusions

A linear model was extracted from the V-22 full nonlinear simulation using LME. This model was verified against time history data from the nonlinear simulation. The linear model accurately represented the lateral-directional dynamics of the verification maneuvers. A second linear model was fit to flight test data using parameter identification tools. This model was verified using an independent maneuver not included in the identification process. The linear model exhibited adequate predictability of the dutch roll mode dynamics.

The lateral-directional dynamic modes of the two linear models were compared. This comparison illustrated a significant difference between the dutch roll modes for the LME and PID models. The stability derivatives for the two models were calculated and compared. The $C_{N\beta}$ derivative was most significantly changed between the two models.

The linear model comparison yielded dynamic mode and stability derivative information unavailable from a standard time history comparison. This information was used to investigate a possible error in the nonlinear simulation math model. Within the scope of this paper, the linear model comparison technique proved to be a valuable tool for validating a complex nonlinear simulation.

Recommendations

The flight test data used in this analysis originated from V-22 envelope expansion flights. The linear model comparison technique could be used more effectively with flight test data better suited to parameter estimation. The control inputs should be excited independently, and maneuvers with small perturbations about the reference condition should be conducted. Multiple maneuvers should be flown to provide sufficient data for identification and verification.

References

[1] Nichols, J. H., "Controls Analysis and Simulation Test Loop Environment (CASTLE) User's Guide CASTLE Version 3.0," Naval Air Warfare Center Aircraft Division, Patuxent River, MD, 1993.

[2] Padfield, G.D., "Simulation Model Validation," AGARD AR-280, 1991, pp. 223-234.

[3] Balderson, Keith and Weathers, Jeffrey, "Comparison of Frequency Response and Perturbation Methods to Extract Linear Models from a Nonlinear Simulation," AIAA Flight Simulation Technologies Conference, 1994.

[4] Etkin, Bernard, "Dynamics of Flight - Stability and Control," John Wiley and Sons, New York, 1982.

[5] McLean, Donald, "Automatic Flight Control Systems," Prentice Hall, New York, 1990.

[6] Maine, Richard E., Iliff, Kenneth W., "Application of Parameter Estimation to Aircraft Stability and Control - The Output Error Approach," NASA RP-1168, 1986.

[7] Grace, Andrew, "Optimization Toolbox User's Guide," The Math Works Inc., 1992.

[8] Pindyck, Robert S., and Rubinfeld, Daniel L., "Econometric Models and Economic Forecasts," McGraw-Hill, Inc., New York, 1991.